This is a repository copy of *Ultrafast Orbital-Oriented Control of Magnetization in Half-Metallic La0.7Sr0.3MnO3 Films*.

White Rose Research Online URL for this paper:
https://eprints.whiterose.ac.uk/id/eprint/161907/

Version: Accepted Version

Ultrafast orbital-oriented control of magnetization in half-metallic La$_{0.7}$Sr$_{0.3}$MnO$_3$ films

Bo Liu,[1] Wei Niu,[1] Yongda Chen,[1] Xuezhong Ruan,[1, *] Zhixiong Tang,[2] Xuefeng Wang,[1, *]

Wenqing Liu,[3] Liang He,[1] Yao Li[1], Jing Wu[4], Shaolong Tang[2], Jun Du[2], Rong Zhang[1], and

Yongbing Xu[1, 4*]

[1]Jiangsu Provincial Key Laboratory of Advanced Photonic and Electronic Materials,

Collaborative Innovation Center of Advanced Microstructures, School of Electronic Science

and Engineering, Nanjing University, Nanjing 210093, P. R. China

[2]Department of Physics, Nanjing University, Nanjing 210093, P. R. China

[3] Department of Electronic Engineering, Royal Holloway, University of London, Egham,

Surrey TW20 0EX, UK

[4]York-Nanjing Joint Center in Spintronics, Department of Electronic Engineering and

Department of Physics, The University of York, York YO10 5DD, UK

*Correspondence Emails: xzruan@nju.edu.cn; xfwang@nju.edu.cn; ybxu@nju.edu.cn

Manipulating spins by ultrafast pulse laser provides a new avenue to switch the magnetization for spintronic applications. While the spin-orbit coupling is known to play a pivotal role in the ultrafast laser-induced demagnetization, the effect of the anisotropic spin-orbit coupling on the transient magnetization remains an open issue. Here, we uncover the role of anisotropic spin-orbit coupling in the spin dynamics in a half-metallic $La_{0.7}Sr_{0.3}MnO_3$ film by ultrafast pump-probe technique. The magnetic order is found to be transiently enhanced or attenuated within the initial sub-picosecond when the probe light is tuned to be s- or p-polarized, respectively. The subsequent slow demagnetization amplitude follows the four-fold symmetry of the $d_{x^2-y^2}$ orbitals as a function of the polarization angles of the probe light. A model based on the Elliott-Yafet spin-flip scatterings is proposed to reveal that the transient magnetization enhancement is related to the spin-mixed states arising from the anisotropic spin-orbit coupling. Our findings provide new insights into the spin dynamics in magnetic systems with anisotropic spin-orbit coupling as well as perspectives for the ultrafast control of information process in spintronic devices.

Since the observation that a femtosecond laser pulse can quench the magnetization in the ferromagnetic Ni film,[1] the field of femtosecond magnetism has attracted great attentions due to the potential advantages of ultra-fast spin manipulation for the advanced data storage.[2-4] One of the key issues related to the ultrafast spin dynamics of magnetic materials is the demagnetization process. In the transition 3d ferromagnetic metals,[5-8] the magnetic order was found to be quenched in a sub-picosecond timescale and then re-magnetized in a longer timescale of several picoseconds (ps). In half metals,[9-11] such as Sr_2FeMoO_6, CrO_2 and $La_{0.6}Sr_{0.4}MnO_3$, experimental observations have shown that the ultrafast demagnetization involves two steps: an initial instantaneous decrease within a ps and a subsequent slow decreasing response lasting for several hundreds of ps. The second step of the slow demagnetization in the half metals is attributed to the spin-lattice relaxation.[9-12] However, in both the 3d transition and half-metallic metals, the microscope origin of the first step of sub-ps demagnetization is still in debate. One of the most prominent mechanisms is the scatterings of various quasiparticles, such as electron-electron, electron-phonon and electron-magnon scatterings.[7,10,13,14] Another completely different explanation for ultrafast demagnetization is the superdiffusive transport of the majority and minority spin polarized electrons.[5,15] Alternatively, Illg et al.[16] claimed that the combination of electron-phonon and electron-magnon scatterings was a possible explanation for ultrafast demagnetization. The above-mentioned momentum-related scattering events involve both the spin and orbit degrees of freedom. For electrons, the spin-orbit interactions (SOI) connect the spin degree of freedom to their orbital motion. Therefore, it is widely believed that spin-orbit interactions (SOI) play an important role in ultrafast demagnetization process as also confirmed by previous X-ray Magnetic Circular Dichroism (XMCD) measurements.[17,18] Hence, utilizing the SOI are expected to allow the control of magnetism in the ultrafast regime.

The colossal magneto-resistive (CMR) materials with half-metallic properties are potential candidates for high efficient spintronic devices and their strong SOI offer the tunability of the couplings between spin, charge, lattice, and orbital degrees of freedom.[19,20] The effect of the anisotropic SOI on the electron transport properties in the CMR manganites is evidenced by the anisotropic magnetoresistance (AMR).[21-23] Recently, the emergence of anisotropic Gilbert damping has been demonstrated in ultrathin Fe layers on GaAs (001) substrate, which is attributed to the anisotropic interfacial SOI.[24] Taking into account the correlation between the damping and relaxation rate of the demagnetization,[13] the anisotropic SOI which determine the Gilbert damping are expected to play a vital role on the ultrafast demagnetization process in the CMR materials. As discussed above, the SOI have been demonstrated to play an important role in the demagnetization process. However, the general issue of the effect of the anisotropic SOI on the temporal magnetization has not been addressed so far. This issue is fundamental to both the understanding of ultrafast demagnetization mechanisms and the optical manipulation of spins in fs/ps time scale.

In this letter, we demonstrate the ultrafast manipulation of the magnetization through the orbital orientation in ferromagnetic $La_{0.7}Sr_{0.3}MnO_3$ (LSMO) thin films by using the time-resolved magneto-optical Kerr effect (TR-MOKE) technique. The ultrafast enhancement or decrease of magnetization within one ps is achieved under s- or p-polarized probe light, respectively. This fast magnetization process correlated with the polarization orientation of the probe light within a ps is explained by a model based on the Elliott-Yafet spin-flip scattering. After this initial fast stage, a slow demagnetization process is then followed, lasting for hundreds of ps. The demagnetization amplitudes under different directions of probe light polarization are found to follow the four-fold symmetry of the orbital order.

The sample studied here with a thickness of 16 nm (40 unit cells) was grown on (001) oriented single crystalline $SrTiO_3$ (STO) terraced substrate. The crystallographic c-axis [001] is normal

to the sample plane. The in-plane crystallographic directions of [100] and [010] are shown in

Figure 1 (a). More details of the growth information are given in the Supplemental Materials

(SM) and other refs.[25,26] The Curie temperature T_C of the film is ~ 334 K (See Figure.S1(a) of

SM). This well resembles the previous results for bulk LSMO,[10,27] indicating the high quality

of the film. In bulk LSMO, the $d_{x^2-y^2}/d_{z^2-y^2}$ orbitals that partially filled by electrons are

responsible for the metallic character and the double-exchange interaction between Mn^{3+} and

Mn^{4+} is responsible for the ferromagnetic order. As the sample exceeds the critical thickness

of 2.5 nm, ferromagnetism is well reserved.[28] The LSMO thin film used in our measurements

exhibits in-plane magnetic anisotropy, which originates from the in-plane tensile strain caused

by the STO substrate. In the epitaxial film, the strain that originated from the substrate may

modify the orbital occupancy.[29] As demonstrated by recent X-ray linear dichroism (XLD)

measurements,[29,30] the tensile strain in LSMO thin film induced by STO substrate implies a

preferential occupancy of the $d_{x^2-y^2}$ orbital. The static Kerr rotation at room temperature is

shown in Figure.S1 (b), showing relatively strong magneto-optical response at high photon

energy. In our pump-probe measurements, 3.1 eV photons were used to probe the sample's

magnetism as indicated by the blue arrow in Figure.S1(b). All the measurements were

performed at room temperature.

The measurement geometry is schematically shown in Figure 1 (a). We used 1.55 eV photons

to excite the sample and the s-polarized 3.1 eV photons to measure the resulting changes of

magnetization. Figure 1 (c) shows the photoinduced change of Kerr rotation $\Delta\theta$ normalized by

the static value θ_0 before optical excitation. After the photoexcitation at $\Delta t = 0$ ps, an

instantaneous increase of $\Delta\theta/\theta_0$ up to 0.15 is observed within 1 ps. Following this

instantaneous increase, the amplitude of $\Delta\theta/\theta_0$ continuously decreases, passes zero at 40 ps,

and finally reaches a minimum of -0.6 at 1.36 ns. Note that the positive sign here represents

the increase of magnetization. Upon the observation of the transient increase of magnetization

with the s-polarized probe beam, the hysteresis loops at different delay-times were measured as shown in Figure 1(d). It clearly shows two reversed types of the transient hysteresis loops at 0.67 ps and 1.36 ns, respectively. These results confirm that, as probed with s-polarized light, an ultrafast increase in magnetization occurs after photoexcitation.

The ultrafast increase in magnetization of perovskite manganites has been reported in several refs.[31-35] The underlying physical mechanisms are fundamentally linked to the density of photogenerated carriers. For example, Yada *et al.*[31] found that the magnetization in $La_{0.9}Sr_{0.1}MnO_3/SrTiO_3$ heterostructures increased within 0.2 ps due to the rapid hole injection from STO into the manganite. Li *et al.*[34] showed a femtosecond generation of ferromagnetic order in $Pr_{0.7}Ca_{0.3}MnO_3$ with photoexcitation threshold behaviour. If the photogenerated carriers dominate the ultrafast increase of magnetism in our sample, then tuning the carrier density will lead to the variation of the ultrafast enhancement. We have conducted one experiment to test this prediction. As shown in Figure2, we extract respectively the amplitudes of the transient hysteresis loops at $\Delta t = 0.67$ ps and 1.36 ns under different pump excitation intensity. The raw data of the transient hysteresis loops under different pump fluence is shown in Figure S2. Clearly, the values at $\Delta t = 0.67$ ps exhibit independence on the pump fluence, demonstrating that the photo-carrier generation does not contribute to this fast magnetization increase.

We notice that the ensuing slow decreasing component in Figure1 (c) is in the ns timescale. This slow magnetization relaxation is associated with the demagnetization due to the increase of the spin temperature by optically heating the spin system through the transferred energy from the equilibrium electron-lattice system. Such spin-lattice relaxation is consistent with previous empirical demagnetization process observed in materials with half-metallic property.[9,10,36,37] In Figure 2, the amplitude of the slow demagnetization component (1.36 ns) increases with increasing pump excitation intensity, which also supports the expectation of the

thermal demagnetization. However, the transient enhancement of the magnetization observed with s-polarized probe light cannot be expected from the thermal process, which should lead to an instantaneous drop rather than increase in magnetization as previously reported.[8] Considering the strongly coupled degrees of freedom between the spin and orbital in the LSMO film, we expect that the orbital orientation plays a role in the magnetization enhancement. To verify this assumption, we have investigated the effect of the probe light polarization orientation on the pump-induced spin dynamics. In Figure 3(a), the recorded temporal trace was measured by the p-polarized probe beam. The polarization orientation and the excitation intensity of the pump beam remain the same as those in Figure 1(c). Under this experimental configuration, the instantaneous change of $\Delta\theta/\theta_0$ within the initial 1 ps points to the negative direction, representing the ultrafast demagnetization. With p-polarized probe beam, the $\Delta\theta/\theta_0$ trace shows a typical two-step demagnetization characteristics, consisting of a step-like decrease and a subsequent slow demagnetization process of hundreds of ps or ns timescale. This observation is consistent with the previous results mentioned above. The transient hysteresis loops at Δt = 30 ps and 1.36 ns shown in Figure 3(b) confirm the in-phase decrease of magnetization. To further study the demagnetization behaviors under different polarization orientations of the probe beam, we have carried out systematic measurements to address this issue. In Figure 3(c), the values of $\Delta\theta/\theta_0$ at time delay of 0.67 ps and 1.36 ns are plotted as a function of the polarization angles of the probe beam. Here, φ = 0° and 90° represent the p- and s-polarization of the probe beam, respectively. The orientation of the s-polarized probe beam aligns with the [010] crystallographic axis of the LSMO thin film. The values of $\Delta\theta/\theta_0$ at 0.67 ps crosses zero at 130°. The sign of the values at 1.36 ns remains the same but their amplitudes change periodically. In Figure 3(d), the demagnetization amplitudes under different probe polarization angles at Δt = 1.36 ns show a four-fold symmetry, which is similar to the occupied $d_{x^2-y^2}$ orbitals as included in Figure 1(b). As experimentally demonstrated by

Buchner et al.,[38] the MOKE method is a powerful tool of probing the interfacial SO coupling by tuning the polarization angle of the probing laser beam. The polarization orientation of the pump beam is found to have no impact on the demagnetization in our measurements (see in Figure S3). This suggests that the pump laser disturbs the sample mainly by the heating effect rather than the electron transition.

The initial quenching of magnetization in half metals has been explained by several models based on the Elliott-Yafet(EY) type spin dependent scattering, such as the electron-electron, electron-phonon or electron-impurity interactions.[14,37,39,40] These microscopic mechanisms are all momentum-dependent scattering events due to the spin-orbit coupling, which would lead to a mixture of the two spin states near the Fermi level. The four-fold symmetry of the demagnetization amplitude at $\Delta t = 1.36$ ns in Figure 3(d) reveals different spin scattering rates along different spatial directions, as expected from the anisotropic spin-orbital coupling in the CMR materials. We have also obtained similar results on two other samples with different thicknesses of 30 and 35 uc, respectively (as shown in Figure S4). The consistent results on different samples support our findings very well. We notice that the anisotropic Gilbert damping in $La_{0.7}Sr_{0.3}MnO_3$ thin film is recently reported,[41] which is ascribed to the anisotropic SO coupling. Similar spin relaxation rates were also reported in other materials arising from the anisotropic spin-orbit coupling.[24,42,43] The fast change of magnetism (~0.67 ps) in Figure 3(c) also has a dependence on probe light polarization orientation, showing different spin scattering rates along various orbital orientations. Note that the polarization of the light can access to different spatial directions of the orbitals.[44,45]

Considering the significant effect of the anisotropic spin-orbit coupling on spin relaxation, we propose a model to explain the observed ultrafast orbital-orientation demagnetization, as shown by the schematic diagram in Figure 4. In the presence of the spin-orbital coupling, an electron state near the Fermi level (straight dash line) is a mixture of the spin-up and spin-down states.[46]

Therefore, a number of spin-down electrons exist in the minority-spin band gap (dash curves in Figure 4). As shown in Figure 4, after photoexcitation by the pump light, non-equilibrium electrons (solid cyan circles) and holes (open circles) with up-spins are generated above and below the E_F, respectively. Since there exist a few spin-down states near the Fermi level, only a small part of the non-equilibrium carriers can be relaxed into the minority empty states via the spin-flip scattering. The p and s polarized probe light correspond to the x and y directions, respectively, as shown in Figure 1(a). Based on the above-mentioned consideration of anisotropic spin-orbit coupling, the photoexcited spin-up electrons prefer the scattering channels along x or y directions, as probed with p- or s-polarized light, respectively. In the case of p-polarized probe light (P process in Figure 4(a)), the spin-up electrons are relaxed into the empty spin-down states via the EY-based spin flip mechanism, leading to an instantaneous decrease of magnetization. For the s-polarized probe light (S process in Figure 4(b)), the electron spin-flip scattering along x direction is prohibited. However, the minority spin-down electrons can recombine with the majority spin-up holes below the Fermi level via the spin-flip scattering along the y direction, leading to an instantaneous increase of the magnetization. In the two processes of S and P, different spin-flip behaviour are necessary to account for the ultrafast demagnetization and remagnetization, respectively. Previous theoretical and experimental studies have suggested specific scattering ways to achieve spin flipping, e.g., electron-phonon, electron-defect and electron-electron scatterings.[14,47-49] As a consequence, the spin angular momentum can be transferred quickly to other degrees of freedom or vice versa. We notice that Wüstenberg et al. have previously revealed the possibility of ultrafast remagnetization via recombination of majority holes and minority electrons in half-metallic Heusler alloy $Co_2Cr_{0.6}Fe_{0.4}Al$ thin films.[50] Their results support ours well. After the initial EY-based instantaneous increase or decrease in magnetization, the spin order of the remaining excited electrons (labeled as slow in Figure 4) is disturbed further via the slow spin-lattice

relaxation channel due to the increasing of the spin temperature. To further demonstrate the effect of orbital-oriented transient magnetization, we have also measured the pump-induced Kerr rotations at time-delays of 0.67 ps and 1.36 ns respectively by rotating the sample orientation angle ϕ with fixed p-polarization of the probe beam. The results obtained by rotating the sample were identical to those obtained by varying the polarization angles of the probe light. The corresponding results are shown in Figure S5 in SM. In the above discussion on the EY-based spin-flip mechanisms, we did not address the specific scattering events (electron-electron, electron-phonon, electron-magnon, or electron-impurity scattering). However, the distinct dependence of the spin order on the orbital orientation suggests that the phonon-mediated scattering events play dominant roles in the sub-ps time scale, which have been reported in previous studies.[37,39,47] We believe that the phenomena of the ultrafast orbital-orientation demagnetization should exist in other ferromagnetic perovskite manganites, where the anisotropic spin-orbital coupling is a general characteristic of this material system.

In summary, the ultrafast orbital-oriented demagnetization process in the thin LSMO film has been studied by the TR-MOKE measurements, which reveals the novel effect of the anisotropic spin-orbit coupling on the temporal magnetization evolution. The transient magnetization enhancement as well as the decrease within the initial 1 ps after photoexcitation has been observed via tuning the polarization orientation of the probe light. A model based on the anisotropic spin-orbit coupling has been proposed to illustrate the spin-flip scattering happening within sub-ps regime. The anisotropic spin-orbit coupling has also been found to induce a four-fold symmetry in the subsequent slowly-relaxed demagnetization process measured by tuning the direction of the probe light polarization. This work has provided new insights into the underlying physics of ultrafast magnetism in the magnetic material systems with anisotropic spin-orbit coupling and new parameters for the ultrafast optical control of the magnetic order.

Experimental Section

The experimental geometry of our TR-MOKE measurement is shown in Figure 1a. The incident pump beam is along the sample normal and the incident angle of the probe beam is around 45° away from the sample normal direction. The femtosecond pulse laser is generated by an amplified Ti: sapphire laser system with a 1 KHz repetition rate, a ~ 50 fs duration time, and a central wavelength of 800 nm (1.55 eV). The majority of the output laser intensity is used to excite the sample as a pump beam. The remainder passing through a BBO crystal is employed to measure the pump induced magnetic variation. The time delay between the two beams is achieved by a mechanical delay stage. The polarization angle of the probe light is tuned by a half-wave plate, as shown in Figure 1a. To obtain the genuine magnetic information, we define $\Delta\theta/\theta_0 = (\Delta\theta_+/\theta_0 - \Delta\theta_-/\theta_0)/2$. Here, $\Delta\theta_+$ and $\Delta\theta_-$ represent the pump-induced Kerr rotations under positive and negative magnetic fields, respectively. θ_0 represents the static Kerr rotation without pump excitation. In the measurements, the sample temperature rise induced by laser illumination was ignored as the time interval between two laser pulses (a millisecond) is long enough for the heat diffusion. One thing that needs to be addressed here is that the raw data in FIG. 3(d) was measured only from $90 - 270°$. The data of $270 - 90°$ was obtained by the four-fold symmetry.

Supporting Information

Supporting Information is available.

Acknowledgements

Conflict of Interest

The authors declare no conflict of interest.

Keywords

Spintronics, ultrafast magnetization, perovskite, spin-orbit coupling, ultrafast spectroscopy
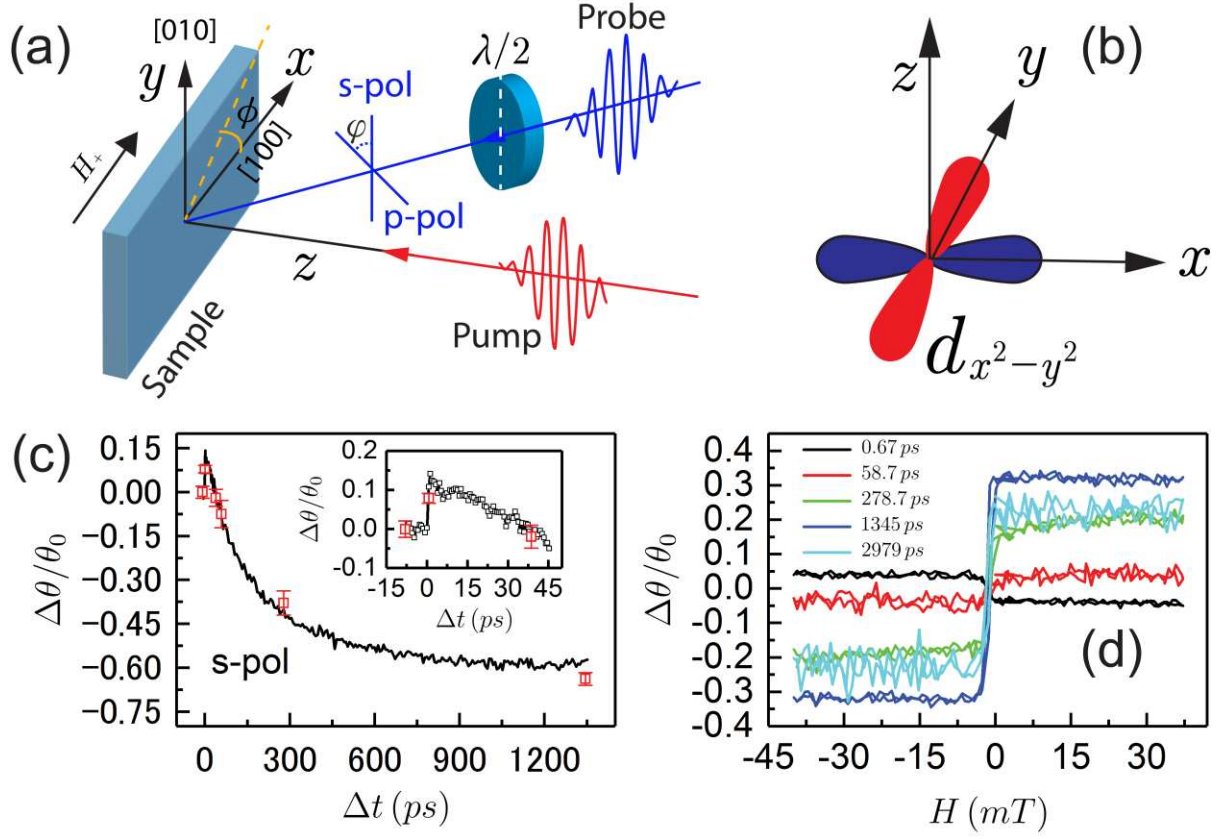
Figure 1. (a) The geometry diagram of the time-resolved magneto-optical Kerr effect. The pump beam is incident perpendicularly on the sample surface. The incident angle of the probe light is 45° with respect to the sample normal direction. A half-wave plate ($\lambda/2$) is used to rotate the polarization plane of the probe light. φ here represents the rotation angle with respect to the incident plane of probe light. In the case of φ = 0°, the electric field of light lies in the plane of the incident probe beam. ϕ is defined as the angle between the spatial x-axis and the crystallographic axis [100] of the LSMO thin film. (b) Diagram of the $d_{x^2-y^2}$ orbitals occupied by the e_g electrons. (c) Temporal characteristics of the pump-induced Kerr rotation with the s-polarized probe beam. The inset shows a magnified view of the ultrafast increase of $\Delta\theta/\theta_0$. (d) The transient hysteresis loops of LSMO film measured at different delay-times. The hysteresis loop probed at 0.67 ps is obviously opposite to those measured at other delay-times. The red squares in (c) represent the amplitude of the transient hysteresis loops at different time delays as shown in (d).
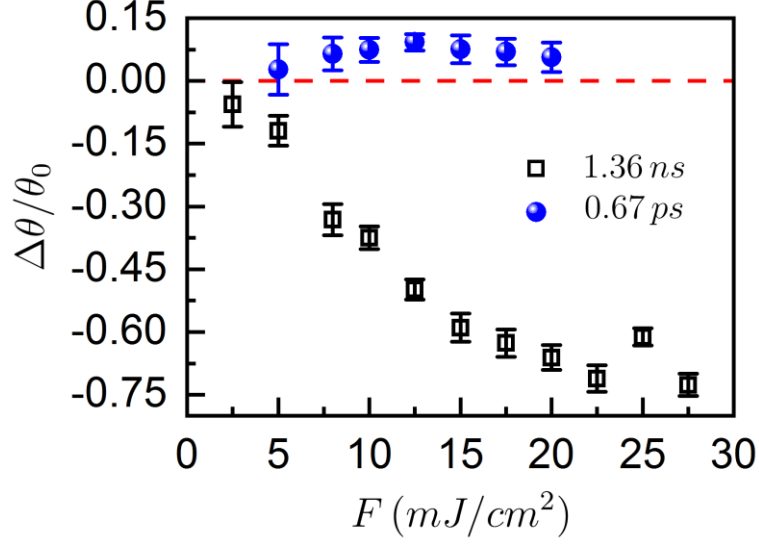
Figure 2. Fluence dependence of the normalized Kerr rotations at different time-delays. The blue and black squares represent the values of $\Delta\theta/\theta_0$ at $\Delta t = 0.67$ ps and 1.36 ns, respectively. The positive sign means the increase of magnetization, while the negative shows the demagnetization. The transient enhancement in magnetization is nearly independent of the pump fluence, while the slow demagnetization component is affected by laser heating.

Figure 3. (a) The time evolution of the pump induced change of Kerr rotation probed with s-polarized probe. Inset: The enlargement of the pump induced Kerr signal at short time window of ~30 ps. (b) Transient hysteresis loops measured at Δt = 30 ps and 1.36 ns. Their amplitude with error bars are shown in (a) at the corresponding time delays. (c) The probe beam polarization orientation dependence of $\Delta\theta/\theta_0$ values at time delays of 0.67 ps and 1.36 ns. The polarization angle of probe beam φ varies from 87° to 180°, corresponding to s and p polarization, respectively. (d) The probe beam polarization orientation dependence of the demagnetization amplitudes at 1.36 ns. The φ is ranged from 0° to 360°. The black and red solid lines in (c) and (d) are guides to the eyes.

Figure 4. (a) The ultrafast magnetization decrease under p-polarized probe. The occupied and unoccupied minority spin density states (green and blank areas) are shown near the Fermi level E_F, which originates from the spin-orbit coupling. The cyan part below the Fermi level is e_g orbits occupied by the majority spins. The red arrows mean the photoexcitation by 1.55 eV pump beam, generating non-equilibrium electrons and holes (cyan and blank circles respectively). The black dash arrow P represents that a part of the excited spin-up electrons is

scattered into the empty spin-down states. Note that the process S is switched off. (b) The schematic process for magnetization increase. Under s-polarized probe, the process P is blocked, while S (solid straight arrow) is switched on. The spin-down electrons in minority electron bands recombine with the excited majority spin-up holes, leading to a transient increase of the magnetism. In both (a) and (b), only a small amount of the excited carriers take part in the fast spin-flip process while the remaining part is relaxed through the slow spin-lattice channel.

Reference

[1]   E. Beaurepaire, J. C. Merle, A. Daunois, J. Y. Bigot, *Phys. Rev. Lett.* **1996**, *76*, 4250.

[2]   J. Walowski, M. Münzenberg, *Journal of Applied Physics* **2016**, *120*, 140901.

[3]   A. Stupakiewicz, K. Szerenos, D. Afanasiev, A. Kirilyuk, A. V. Kimel, *Nature* **2017**, *542*, 71.

[4]   Y. Xu, M. Deb, G. Malinowski, M. Hehn, W. Zhao, S. Mangin, *Advanced Materials* **2017**, *29*, 1703474.

[5]   N. Bergeard, M. Hehn, S. Mangin, G. Lengaigne, F. Montaigne, M. L. M. Lalieu, B. Koopmans, G. Malinowski, *Phys. Rev. Lett.* **2016**, *117*, 147203.

[6]   B. Koopmans, van Kampen M, J. T. Kohlhepp, W. J. M. de Jonge, *Journal of Applied Physics* **2000**, *87*, 5070.

[7]   E. Carpene, E. Mancini, C. Dallera, M. Brenna, E. Puppin, S. De Silvestri, *Phys Rev B* **2008**, *78*, 174422.

[8]   J.-H. Shim, A. Ali Syed, C.-H. Kim, K. M. Lee, S.-Y. Park, J.-R. Jeong, D.-H. Kim, D. Eon Kim, *Nature Communications* **2017**, *8*, 796.

[9]   T. Kise, T. Ogasawara, M. Ashida, Y. Tomioka, Y. Tokura, M. Kuwata-Gonokami, *Phys. Rev. Lett.* **2000**, *85*, 1986.

[10]   T. Ogasawara, K. Ohgushi, Y. Tomioka, K. S. Takahashi, H. Okamoto, M. Kawasaki, Y. Tokura, *Phys. Rev. Lett.* **2005**, *94*, 087202.

[11]   Q. Zhang, A. V. Nurmikko, G.-X. Miao, G. Xiao, A. Gupta, *Phys Rev B* **2006**, *74*, 064414.

[12]   G. M. Müller, J. Walowski, M. Djordjevic, G.-X. Miao, A. Gupta, A. V. Ramos, K. Gehrke, V. Moshnyaga, K. Samwer, J. Schmalhorst, A. Thomas, A. Hütten, G. Reiss, J. S. Moodera, M. Münzenberg, *Nat Mater* **2009**, *8*, 56.

[13]   B. Koopmans, J. J. M. Ruigrok, F. D. Longa, W. J. M. de Jonge, *Phys.*

Rev. Lett. **2005**, *95*, 267207.

[14] M. Krauß, T. Roth, S. Alebrand, D. Steil, M. Cinchetti, M. Aeschlimann, H. C. Schneider, *Phys Rev B* **2009**, *80*, 180407.

[15] A. J. Schellekens, W. Verhoeven, T. N. Vader, B. Koopmans, *Appl. Phys. Lett.* **2013**, *102*, 252408.

[16] C. Illg, M. Haag, M. Fähnle, *Phys Rev B* **2013**, *88*, 152.

[17] C. Boeglin, E. Beaurepaire, V. Halté, V. López-Flores, C. Stamm, N. Pontius, H. A. Dürr, J. Y. Bigot, *Nature* **2010**, *465*, 458.

[18] C. Stamm, T. Kachel, N. Pontius, R. Mitzner, T. Quast, K. Holldack, S. Khan, C. Lupulescu, E. F. Aziz, M. Wietstruk, H. A. Dürr, W. Eberhardt, *Nat Mater* **2007**, *6*, 740.

[19] F. Li, C. Song, Y. D. Gu, M. S. Saleem, F. Pan, *Phys Rev B* **2017**, *96*, 245108.

[20] F. Li, C. Song, B. Cui, J. Peng, Y. Gu, G. Wang, F. Pan, *Advanced Materials* **2017**, *29*, 1604052.

[21] R.-W. Li, H. Wang, X. Wang, X. Z. Yu, Y. Matsui, Z.-H. Cheng, B.-G. Shen, E. W. Plummer, J. Zhang, *Proc Natl Acad Sci USA* **2009**, *106*, 14224.

[22] P. Perna, D. Maccariello, F. Ajejas, R. Guerrero, L. Méchin, S. Flament, J. Santamaria, R. Miranda, J. Camarero, *Advanced Functional Materials* **2017**, *27*, 1700664.

[23] J.-B. Yau, X. Hong, A. Posadas, C. H. Ahn, W. Gao, E. Altman, Y. Bason, L. Klein, M. Sidorov, Z. Krivokapic, *Journal of Applied Physics* **2007**, *102*, 103901.

[24] L. Chen, S. Mankovsky, S. Wimmer, M. A. W. Schoen, H. S. Körner, M. Kronseder, D. Schuh, D. Bougeard, H. Ebert, D. Weiss, C. H. Back, *Nature Physics* **2018**, *26*, 1366.

[25] W. Niu, M. Gao, X. Wang, F. Song, J. Du, X. Wang, Y. Xu, R. Zhang, *Scientific reports* **2016**, *6*, 26081.

[26] W. Niu, X. Wang, M. Gao, Z. Xia, J. Du, Y. Nie, F. Song, Y. Xu, R. Zhang, *AIP Advances* **2016**, *7*, 056404.

[27] A. M. Haghiri-Gosnet, J. P. Renard, *J Phys D Appl Phys* **2003**, *36*, R127.

[28] M. Huijben, L. W. Martin, Y. H. Chu, M. B. Holcomb, P. Yu, G. Rijnders, D. H. A. Blank, R. Ramesh, *Phys Rev B* **2008**, *78*, 094413.

[29] D. Pesquera, G. Herranz, A. Barla, E. Pellegrin, F. Bondino, E. Magnano, F. Sánchez, J. Fontcuberta, *Nature Communications* **2012**, *3*, 1189.

[30] B. Wang, L. You, P. Ren, X. Yin, Y. Peng, Bin Xia, L. Wang, X. Yu, S. M. Poh, P. Yang, G. Yuan, L. Chen, A. Rusydi, J. Wang, *Nature Communications* **2013**, *4*, 2778.

[31] H. Yada, M. Matsubara, H. Yamada, A. Sawa, H. Matsuzaki, H. Okamoto, *Phys Rev B* **2011**, *83*, 165408.

[32] H. Yada, M. Matsubara, H. Matsuzaki, H. Yamada, A. Sawa, H.

Okamoto, *Phys Rev B* **2011**, *84*, 045114.

[33] M. Matsubara, A. Schroer, A. Schmehl, A. Melville, C. Becher, M. Trujillo-Martinez, D. G. Schlom, J. Mannhart, J. Kroha, M. Fiebig, *Nature Communications* **2015**, *6*, 6724.

[34] T. Li, A. Patz, L. Mouchliadis, J. Yan, T. A. Lograsso, I. E. Perakis, J. Wang, *Nature* **2013**, *496*, 69.

[35] S. Koshihara, A. Oiwa, M. Hirasawa, S. Katsumoto, Y. Iye, C. Urano, H. Takagi, H. Munekata, *Phys. Rev. Lett.* **1997**, *78*, 4617.

[36] A. I. Lobad, R. D. Averitt, C. Kwon, A. J. Taylor, *Appl. Phys. Lett.* **2000**, *77*, 4025.

[37] B. Koopmans, G. Malinowski, F. D. Longa, D. Steiauf, M. Fähnle, T. Roth, M. Cinchetti, M. Aeschlimann, *Nat Mater* **2009**, *9*, 259.

[38] M. Buchner, P. Högl, S. Putz, M. Gmitra, S. Günther, M. A. W. Schoen, M. Kronseder, D. Schuh, D. Bougeard, J. Fabian, C. H. Back, *Phys. Rev. Lett.* **2016**, *117*, 565.

[39] K. Carva, M. Battiato, P. M. Oppeneer, *Phys. Rev. Lett.* **2011**, *107*, 207201.

[40] K. Leckron, S. Vollmar, H. C. Schneider, *Phys Rev B* **2017**, *96*, 140408.

[41] Q. Qin, S. He, H. Wu, P. Yang, L. Liu, W. Song, S. J. Pennycook, J. Chen, *arXiv* **2018**, *cond-mat.mtrl-sci*.

[42] T. Wakamura, F. Reale, P. Palczynski, S. Guéron, C. Mattevi, H. Bouchiat, *Phys. Rev. Lett.* **2018**, *120*, 106802.

[43] L. A. Benítez, J. F. Sierra, W. Savero Torres, A. Arrighi, F. Bonell, M. V. Costache, S. O. Valenzuela, *Nature Physics* **2017**, *14*, 303.

[44] C. Jozwiak, C.-H. Park, K. Gotlieb, C. Hwang, D.-H. Lee, S. G. Louie, J. D. Denlinger, C. R. Rotundu, R. J. Birgeneau, Z. Hussain, A. Lanzara, *Nature Physics* **2013**, *9*, 293.

[45] C. Jozwiak, J. A. Sobota, K. Gotlieb, A. F. Kemper, C. R. Rotundu, R. J. Birgeneau, Z. Hussain, D.-H. Lee, Z.-X. Shen, A. Lanzara, *Nature Communications* **2016**, *7*, 13143.

[46] B. Casals, R. Cichelero, P. García Fernández, J. Junquera, D. Pesquera, M. Campoy-Quiles, I. C. Infante, F. Sánchez, J. Fontcuberta, G. Herranz, *Phys. Rev. Lett.* **2016**, *117*, 026401.

[47] S. Essert, H. C. Schneider, *Phys Rev B* **2011**, *84*, 224405.

[48] B. Koopmans, H. H. J. E. Kicken, van Kampen M, W. J. M. de Jonge, *Journal of Magnetism and Magnetic Materials* **2005**, *286*, 271.

[49] D. Steil, S. Alebrand, T. Roth, M. Krauß, T. Kubota, M. Oogane, Y. Ando, H. C. Schneider, M. Aeschlimann, M. Cinchetti, *Phys. Rev. Lett.* **2010**, *105*, 217202.

[50] J.-P. Wüstenberg, D. Steil, S. Alebrand, T. Roth, M. Aeschlimann, M. Cinchetti, *physica status solidi (b)* **2011**, *248*, 2330.